# D region Ionospheric Imaging Using VLF/LF Broadband Sferics, Forward Modeling, and Tomography

Jackson C. McCormick and Morris B. Cohen
Electrical and Computer Engineering
Georgia Institute of Technology
Atlanta, Georgia
jcmccorm@gatech.edu

Abstract— The D region of the ionosphere (60-90 km) is very important for a variety of radio science applications. It is utilized in important applications as it reflects Very Low Frequency (VLF, 3-30 kHz) waves, ranging from navigation to communication to lighting geolocation. However, despite the large body of D region applications and research, we still know relatively little about the underlying structure. This is in large part due to the difficulty of making direct measurements, which is why many workers have utilized the same VLF waves to perform remote sensing studies. However, noticeably absent in the field, is a thorough study which attempts to recover a map of the D region. We describe possible methods to utilize the broadband VLF emissions from lightning and a receiver network to obtain a 2D ionospheric map using methods from Compressed Sensing (CS) and Computed Tomography (CT).

### Keywords—D region; ionosphere; lightning; imaging

## I. INTRODUCTION

The D region of the ionosphere (60-90 km) is an important but relatively poorly understood region. Due to the collisional nature of the D region plasma, HF (3-30 MHz) waves propagating through it are significantly attenuated. The D region efficiently reflects VLF and LF (3-30/30-300 kHz) waves, trapping them between the earth and the D region ionosphere forming what is known as the Earth-Ionosphere Waveguide (EIWG). Scientifically, this is fortunate because it is otherwise very difficult to make measurements at altitudes too high for balloons but too low for satellites.

Because of the efficient propagation of VLF waves to global lengths in the EIWG, in addition to the relatively large skin depth for VLF frequencies in salt water, navies have constructed VLF transmitters operating at high power for nearly continuous submarine communication. Many researchers have utilized these VLF beacons to study the D region of the ionosphere in a

remote sensing manner [Thomson, 1993; Bainbridge and Inan, 2003, Gross et al. 2018]. Because the transmitters operate with a small bandwidth, they are commonly referred to as 'narrowband' signals. In addition to the narrowband signals, the return stroke lightning is an impulsive radiator of a VLF/LF radio wave packet known as a 'sferic' which has been utilized to study the D region [Cummer et al. 1998, Shao et al., 2013]. Lightning is spread globally throughout 600-700 storms [Hutchins et al., 2014] and occurs ~40-50 times per second [Christian et al., 2003], opening up a greater opportunity for spatial studies of the D region. However, some difficulties exist in using lightning for remote sensing such as the variance of current sources and lightning channel geometry from source to source. Recently, McCormick et al. [2018 (In Review)] demonstrated a technique to adjust for the variability in the lightning source in addition to recovering phase measurements, recovering a second component to the magnetic field, and combining sferics from many strokes at the same locations to boost the SNR of the measurement. These processing steps potentially allow the utilization of the entire global distribution of lightning.

Since the development and demonstration of Computed Tomography (CT) for medical use by Hounsfield [1973], there has been an explosion of research in medical CT applications (e.g. PET, SPECT, MRI). CT has proven important for other applications where direct in-situ measurements are difficult or impossible, such as ionospheric studies in the E and F regions of the ionosphere (100-500 km) [Yao et al., 2014]. However, despite early discussions of the potential use of lightning to study the D region ionosphere using CT principles [Cummer et al. 1998], we are unaware of any attempts to date. In short, no one has been able to produce a real 'map' of the D region, such as what exists for the F region via, for example, GPS remote sensing.

Perhaps the lack of results is due to challenges with the measurement setup of the D region and lightning tomography. In tomographic techniques, measurements are typically made with roughly even distribution around the outside of a region to be imaged. On the other hand, the problem we face of ionospheric estimation involves sources and receivers that exist within the region to be studied, and are somewhat randomly distributed. The measurement geometry renders the well-developed inversion techniques used in CT, such as Filtered Back Projection (FBP), unusable. There is also a family of 'iterative' techniques for tomographic problems that may be useful in D region CT studies, but unfortunately, resolving the D region at a reasonably fine scale will almost always lead to an ill-conditioned problem.

Motivated by the idea of making imaging systems more efficient, Candès et al. [2006 (and references therein)] developed the Compressed Sensing (CS) technique. CS allows for acquisition and imaging of signals with less samples than required by the Shannon-Nyquist sampling requirement by taking advantage of the concept of sparseness. By exploiting sparseness in the D region imaging, it may become possible to acquire an image despite the difficulties present in the raw imaging setup.

#### II. EXPERIMENTAL SETUP

We utilize continuous magnetic field time-series VLF/LF data (~1-50 kHz) acquired from an instrument similar to the AWESOME instrument as described by [Cohen et al., 2010]. The system consists of two orthogonal wire loop antennas mounted in the North/South and East/West directions. Sampled data is referenced to GPS time with an absolute timing accuracy of ~15-20 ns. The receiver represented in the example in Figure 1 is located in Baxley, GA, USA (N31.8767, W82.3620).

To interpret the received and processed sferics, we use the Long Wave Propagation Capability (LWPC) program [Ferguson, 1998] developed by the US navy to predict narrowband propagation. LWPC divides a source-receiver path into discrete slabs, allowing for the specification of important waveguide parameters such as the electron density in the D region, and ground conductivity/permittivity. In order to reduce the dimensionality of the problem, we follow the Wait and Spies [1964] two parameter electron density parameterization, where h' is interpreted as the effective reflection height, and  $\beta$  can be seen as the gradient of the electron density.

$$N_e = 1.43 * 10^7 \exp(-\dot{0}.15h') * \exp[(\beta - 0.15)(h - h')] cm^{-3}$$
 (1)

By simulating all frequencies with a phase delay corresponding to an upward propagating current waveform (from ground to cloud) and summing the solution together, we can predict sferic waveform propagation. We determine the best fit D region parameters by simulating over many possible h',  $\beta$  combinations and comparing to the received sferic waveform from 5-30 kHz with the L<sub>2</sub> norm. We interpret the inferred h',  $\beta$  parameters to be the path-averaged information. The cost function for a typical example along with the matched waveform and some diverging examples are shown in Figure 1. The uniqueness of the fit as seen in the cost function gives us confidence that our path-average inferences are correct.

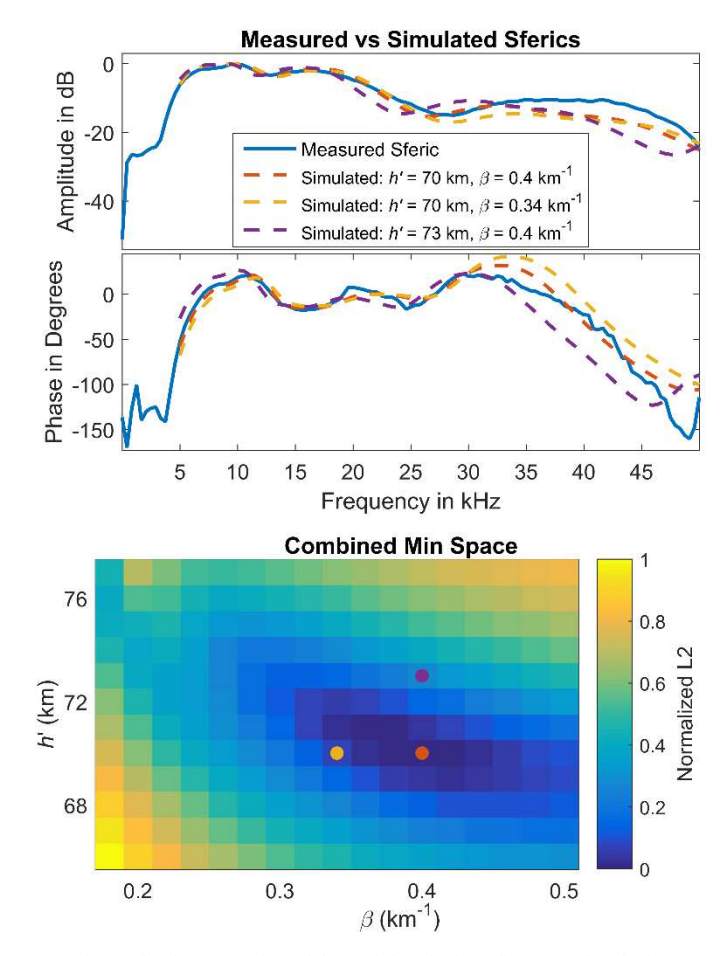


Fig 1. The demonstration of determining the best-fit h',  $\beta$  pair. The bottom panel shows the cost surface when normalizing and weighing the phase and amplitude data equally. The top and middle panel demonstrate measured and processed example sferic amplitude and phase along with some example simulated results. The colors correspond to the location in the cost function with the red results corresponding to the best-fit.

McCormick et al. [2018 (In Review)] empirically determined that ~10 lightning strokes of sufficient quality were needed to reproduce a high quality representative sferic waveform. Lightning strokes follow certain meteorological trends, but their exact locations tend to be randomly distributed. Therefore, the example in Figure 2 is an example of a typical dataset available for D region CT image reconstruction, but the actual geometry varies greatly. It is clear that the sources are clustered around storm systems, but still are geographically diverse.

# III. FORMULATION AND DISCUSSION

For typical CT setups, the problem can be thought of as the typical  $\mathbf{y} = \mathbf{A}\mathbf{x}$  linear algebra formulation, where  $\mathbf{y}$  is the observed line-integrals (path-averaged ionospheric inferences times the length of that respective path) and  $\mathbf{x}$  is the vectorized unknown ionospheric image. A is the system model with each row being an observation, with information on pixels that are traversed by a source-receiver path.

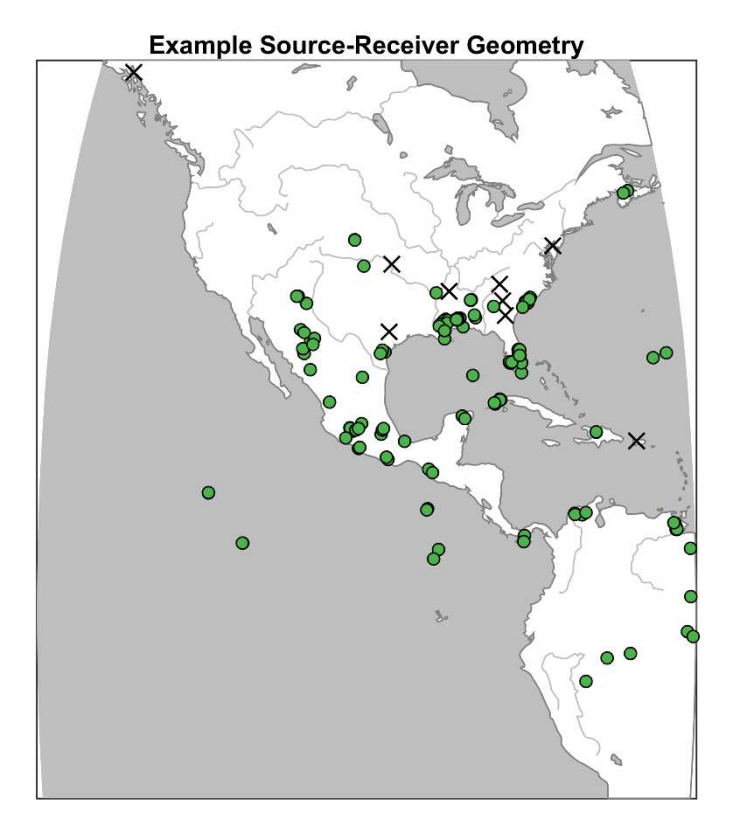


Fig 2. An example of typical lighting-source and receiver geometry. The receivers are plotted as black crosses representing the active receiver network operated by the Georgia Tech LF group. The green dots are a proxy for a cluster of  $\sim$ 10 strokes each. The 180 green dots, therefore, symbolize 180 representative and processed sferics (reduced from the whole dataset of 1800). All the strokes pictured occurred from 20:30:00-20:31:00 UT.

However, when finer details are desired and pixels sized reduced, the problem will quickly become ill-conditioned. Therefore, we need some way to approach a problem with the given undersampled dataset. Previous workers [Jorgenson et al., 2012 (and references therein)] solved similar problems by integrating the principles of CS, namely by taking sparse characteristics of the image to be reconstructed or the image after applying a sparsifying transform. This idea can be expressed mathematically as a constrained minimization problem:

$$x = \min \|\psi(x)\|_0 \text{ such that } Ax = y \tag{2}$$

Where  $\psi(.)$  is the sparsifying transform and  $\|.\|_0$  is the  $L_0$  psuedonorm calculated by taking the number of non-zero terms. However, this system is rarely directly solved because it is very computationally burdensome to directly solve the  $L_0$  psuedonorm. Therefore, many CS systems prescribe using the  $L_1$  norm instead.

In order to solve the system, we need to determine or design some sort of transform that will sparsify the system. Some take advantage of the Total Variation (TV) norm in some way, which measures the total gradient of the image. When used in a minimization problem, it has the effect of causing piecewise constant images, allowing for sharp edges. However, this may not be very helpful in describing the D-region ionosphere, since it would tend to smooth out all bumps, while preserving sharp edges that may only exist at the day-night terminator.

While no D region image or map has been produced, many perturbations and structural changes have been observed and modeled. During the nighttime, D region lightning can cause both direct ionospheric perturbations caused by the lightning electromagnetic pulse or quasi-electrostatic field induced ionization known as Early/Fast events [Inan et al., 1991], lasting tens of minutes and tens of km in extent. It can also cause indirect particle precipitation caused by lightning energy interacting with the electrons in radiation belts called Lightning-Induced Electron Precipitation (LEP) [Helliwell et al., 1973], lasting tens of seconds to minutes and hundreds of km in extent.

It is clear is that a sparsifying transform that will make a meaningful impact on the D region imaging approach. It could, for example, take advantage of the typical smoothness of the D region by allowing for smooth, but pronounced perturbations. Furthermore, the ionosphere is a dynamic system, thus a robust approach must take the time-evolution into account. A robust method that allows for future updates, while taking past estimates into account is the Kalman filter, which will allow for flexibility for future updates and a time-evolving D region ionosphere.

#### IV. CONCLUSION AND FUTURE WORK

The D region ionosphere has been the subject of countless studies and papers. However, most VLF/LF remote sensing studies are limited by the fact that waveguide codes tend to infer path-averaged information about the D region. There may be an opportunity to infer a D region image by utilizing observations of global lightning-generated VLF sferics. To approach the problem, we need a dense set of sources and receivers to be able to solve for the underlying image. We discussed potential approaches of how to utilize the full set of lightning data along with modern Compressed Sensing and Computed Tomography techniques. Lastly, we discussed how to constrain the problem based on aspects of D-region perturbations and structure.

#### REFERENCES

Bainbridge, G., and U. S. Inan (2003), Ionospheric D region electron density profile derivednfrom the measured interference pattern of VLF waveguide modes, Radio Science, 38(4), doi:10.1029/2002RS002686.

Candès, E. J., J. K. Romberg, and T. Tao (2006), Stable signal recovery from incomplete and inaccurate measurements, Communications on Pure and Applied Mathematics, 59(8), 1207–1223, doi:10.1002/cpa.20124.

Christian, H. J., R. J. Blakeslee, D. J. Boccippio, W. L. Boeck, D. E. Buechler, K. T. Driscoll, S. J. Goodman, J. M. Hall, W. J. Koshak, D. M. Mach, and M. F. Stewart (2003), Global frequency and distribution of lightning as observed from space by the Optical Transient Detector, J. Geophys. Res., 108(D1), ACL 4–1—ACL 4–15.

Cohen, M. B., U. S. Inan, and E. W. Paschal (2010), Sensitive Broadband ELF/VLF Radio Reception With the AWESOME Instrument, IEEE Transactions on Geoscience and Remote Sensing, 48(1).

Cummer, S. A., U. S. Inan, and T. F. Bell (1998), Ionospheric D region remote sensing using VLF radio atmospherics, Radio Science, 33(6), 1781–1792.

Ferguson, J. A. (1998), Computer Programs for Assessment of Long-Wavelength Radio Communications, Tech. Rep. 3030, Space and Naval Warfare Systems Center, San Diego.

Gross, N. C., M. B. Cohen, R. K. Said, and M. Gołkowski (2018), Polarization of Narrowband VLF Transmitter Signals as an Ionospheric Diagnostic, Journal of Geophysical Research: Space Physics, pp. n/a—n/a, doi:10.1002/2017JA024907.

- Helliwell, R. A., J. P. Katsufrakis, and M. L. Trimpi (1973), Whistler-Induced Amplitude Perturbation in VLF Propagation, Journal of Geophysical Research, 78(22), 4679–4688.
- Hounsfield, G. N. (1973), Computer transverse axial scanning (tomography). Part I. Description of system., British Journal of Radiology, 46(1016).
- Hutchins, M. L., R. H. Holzworth, and J. B. Brundell (2014), Diurnal variation of the global electric circuit from clustered thunderstorms, J. Geophys. Res. Space Physics, 119(1), 620–629.
- Inan, U. S., T. F. Bell, and J. V. Rodriguez (1991), Heating and ionization of the lower ionosphere by lightning, Geophysical Research Letters, 18(4), 705–708
- Jorgensen, J. S., E. Y. Sidky, and X. Pan (2013), Quantifying Admissible Undersampling for Sparsity-Exploiting Iterative Image Reconstruction in X-Ray CT, IEEE Transactions on Medical Imaging, 32(2), 460–473, doi:10.1109/TMI.2012.2230185.

- McCormick, J. C., M. B. Cohen, N. C. Gross, and R. K. Said (2018), Spatial and temporal ionospheric monitoring using broadband sferic measurements, Journal of Geophysical Research, Space Physics.
- Shao, X.-M., E. H. Lay, and A. R. Jacobson (2013), Reduction of electron density in the night-time lower ionosphere in response to a thunderstorm, Nature Geosci, 6(1), 29–33.
- Thomson, N. R. (1993), Experimental daytime VLF ionospheric parameters, Journal of Atmospheric and Terrestrial Physics, 55(2), 173–184.
- Wait, J. R., and K. P. Spies (1964), Characteristics of the earth-ionosphere waveguide for VLF radio waves, Technichal Note 300, National Bureau of Standards.
- Yao, Y., J. Tang, P. Chen, S. Zhang, and J. Chen (2014), An improved iterative algorithm for 3-D ionospheric tomography reconstruction, IEEE Transactions on Geoscience and Remote Sensing, 52(8).